Cement and Concrete Research 38 (2008) 1126–1129

Contents lists available at ScienceDirect

Cement and Concrete Research

journal homepage: http://ees.elsevier.com/CEMCON/default.asp

Discussion

Does C–S–H particle shape matter? A discussion of the paper 'Modelling elasticity of a hydrating cement paste', by Julien Sanahuja, Luc Dormieux and Gilles Chanvillard. CCR 37 (2007) 1427–1439

Franz-Josef Ulm [a,*], Hamlin M. Jennings [b]

[a] Massachusetts Institute of Technology, Cambridge, MA, United States
[b] Northwestern University, Evanston, Ill., United States

ARTICLE INFO

Article history:
Received 11 December 2007
Accepted 30 March 2008

Keywords:
Calcium–silicate–hydrate (C–S–H)
Microstructure
Micromechanics
Nanoindentation
SANS

ABSTRACT

In their inspiring paper, Sanahuja et al. (CCR (37) 1427–1439) add a new dimension and degree of freedom for implementing the Materials Science Paradigm between microstructure and properties of cement-based materials, which is the particle aspect ratio of C–S–H elementary building block. The question addressed in this discussion is how far this departure from the perfect disordered morphology of C–S–H is truly relevant for cement-based materials.

1. Introduction

Implementing the materials science paradigm between microstructure and properties for cementitious materials continues to be a formidable challenge in materials science and engineering mechanics. This is no doubt due to the high heterogeneity of the material and its many pore spaces that manifest themselves from the nanoscale to the macroscale. In this quest, Sanahuja et al. (CCR (37) 1427–1439) add a new dimension and degree of freedom for modeling the problem, which is the percolation threshold of C–S–H elementary building block. Based on advanced micromechanics analysis, the authors first derive and then apply to cement paste at early ages, a relationship between the percolation threshold, which is the volume fraction of particles required to form a continuous force path through the system, and particle shape.

The packing of particles is a focus of attention in the granular physics community, and several researchers have attempted to understand packings of ellipsoids. Onoda and Liniger [1] determined that the random-loose packing fraction of uniform spheres at the limit of zero gravitational force is 0.555±0.005, which corresponds to a sphere packing at its rigidity-percolation threshold. Buchalter and Bradley [2] performed Monte Carlo simulations of the pouring of oblate and prolate ellipsoids, and showed that increased asphericity (prolate and oblate) yields lower percolation thresholds. Similar results have been obtained by Coelho et al. [3] and Sherwood [4] using a sequential deposition algorithm of rigid particles of different shapes. The finding of Sanahuja et al., therefore, is quantitatively in very good agreement with granular physics results, as shown in Fig. 1 (which reproduces results of Sanahuja et al. (Fig. 6) together with the here cited references of granular physics). This confirms, if need still be, that the self-consistent model of linear micromechanics, which originated independently from Hershey [5] and Kröner [6], recognizes the percolation threshold associated with granular materials. Kröner's original work considered a perfectly random distribution of contact surfaces between particles. This averaged random contact may be represented, mechanically, by a sphere. For the spherical case, the percolation threshold of the polycrystal model is η_0=0.5. While a sphere itself is a 'perfectly disordered' particle shape in the context of the self-consistent model [7], non-spherical shapes introduce some order to the system, leading to a percolation threshold below η_0<0.5.

The question we want to address in this discussion is how far from the percolation threshold of 0.5, and thus from the perfect disorder in both properties and morphology, can be this departure while remaining truly relevant for cement-based materials.

2. A look back on macroscopic data

In an attempt to implement the materials science paradigm for cement-based materials, the cement science and engineering literature, not surprisingly, is rich in macro-property–porosity relationships. As an example, from plotting the cube strength vs. capillary porosity (pores greater than about 1 nm according to some

* Corresponding author.
E-mail address: ulm@MIT.EDU (F.-J. Ulm).

0008-8846/$ – see front matter © 2008 Elsevier Ltd. All rights reserved.
doi:10.1016/j.cemconres.2008.03.023

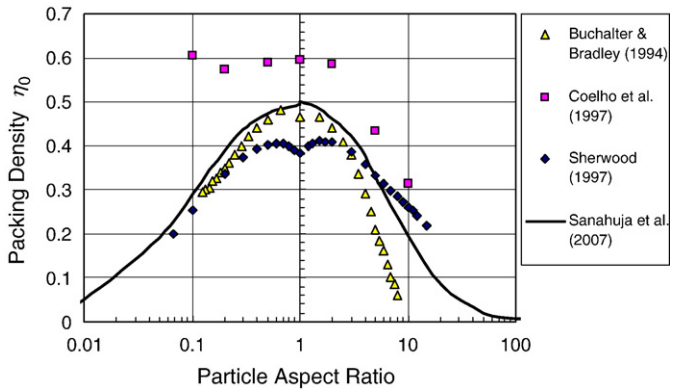

Fig. 1. Percolation threshold vs. particle aspect ratio predicted by the (continuum micromechanics) Self-consistent scheme and granular physics discrete approaches: Data from Buchalter and Bradley [2] were generated from Monte Carlo simulations of the pouring of oblate and prolate ellipsoids in a container. Packings from Sherwood [4] were obtained by random sequential deposition simulations of oblate and prolates at the jamming limit. Data from Coelho et al. [3] are also obtained by a random sequential deposition algorithm of non-overlapping grains with ellipsoidal shape. Data from Sanahuja et al. obtained with the self-consistent scheme of continuum micromechanics.

definitions) Verbeck and Helmuth [8] concluded in a 1969 conference paper that cement paste strength depends on capillary porosity (Fig. 2 (*a*)). The capillary porosity reported in the graph includes most of the gel pores (except for a few younger age samples, which probably contained some true capillary pores). Remarkably, a straight line fit of the data to a zero strength gives an estimate of $\eta_0 \approx 0.5$ for the percolation threshold, hinting towards a random morphology of the hydration products in the hardened material. In other words, if C–S–H had a distinct oblate particle shape, this particle shape would have little influence on the scaling of cement paste strength with the porosity in the porosity range of $0 \le \phi_0 \le 40\%$. This is the porosity range the most relevant for hardened cementitious materials.

3. C–S–H density, nanoindentation modulus and hardness and SANS results

Correlating C–S–H density measurements and nanoindentation results provides a second means to check the relevance of a micromechanical amorphous vs. a shape-driven mechanical morphology of the C–S–H hydration products. This is shown in Fig. 2 in which values of indentation modulus (Fig. 2(*b*)) and indentation hardness (Fig. 2(*c*)) of the Low-Density (or outer products) and the High Density (or inner products) C–S–H structures obtained from statistical nanoindentation technique [9], are plotted vs. C–S–H values of packing density obtained from mass density measurements, small-angle neutron scattering (SANS) and X-ray scattering data [10–12]. The overall picture that emerges is one of a nanogranular material possessing a percolation threshold on the order of $\eta_0 = 0.5$, reminiscent of the self-consistent theory with perfect sphericity. The characteristic packing densities of LD and HD C–S–H calculated from density, i.e. $\eta_{LD} = 0.65$ and $\eta_{HD} = 0.73$ (instead of $\eta_{HD} = 0.7$ assumed by Sanahuja et al. to estimate an unreasonably high C–S–H particle stiffness compared with e.g. results of atomistic simulation [13]), come remarkably close to *limit* packing densities of spheres, namely the random close-packed limit (RCP, [14]) or maximally random jammed state (MRJ, [15]) of $\eta \approx 0.64$; and the ordered face-centered cubic (fcc) or hexagonal close-packed (hcp) packing of $\eta = \pi/\sqrt{18} \approx 0.74$ [16]. Arguably, one could equally achieve similar high packings with ellipsoids of different aspect ratios (but not with oblates or prolates) [15]. Yet, the higher the density the lower the aspect ratio required to achieve a jammed disordered configuration. The percolation threshold of $\eta_0 = 0.5$, therefore, ascertains a perfectly disordered morphology as being most likely represented by packed spheres. In favor of this spherical morphology are data obtained by SANS which unlike most observations on the structure of C–S–H, examines fully saturated pastes. In fact, the model for LD and HD C–S–H microstructure (which the authors employ), keys on data from SANS, which fits the scattering vector to intensity over a wide range of length scales [17]. The size of

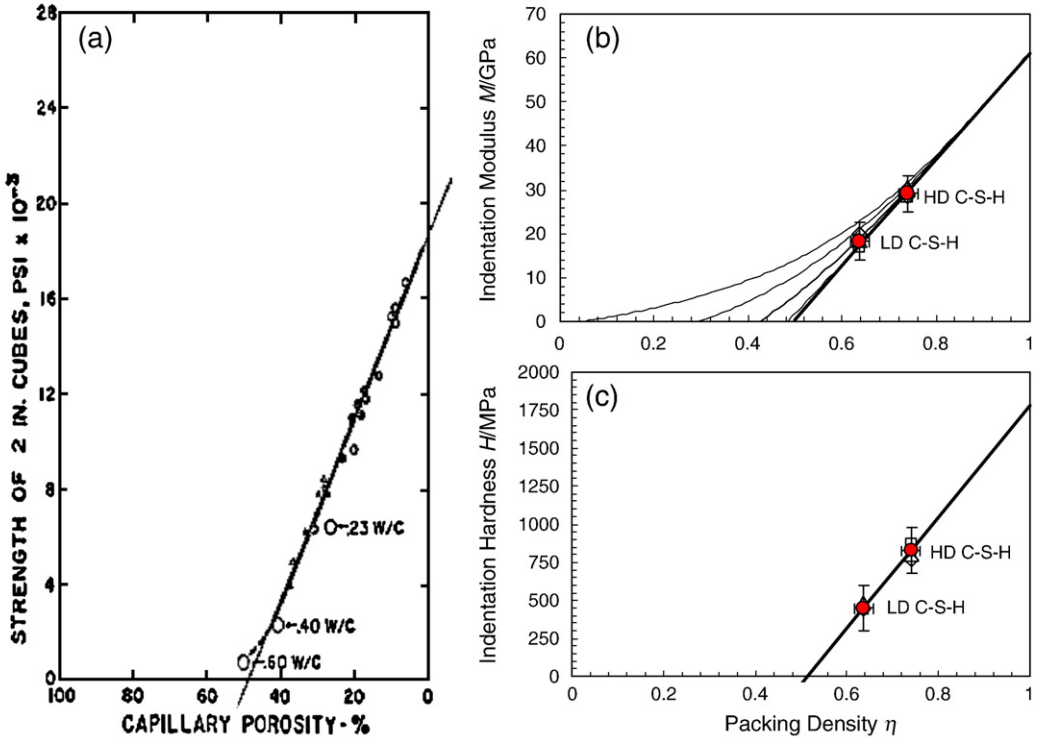

Fig. 2. Evidence of $\eta_0 \approx 0.5$ percolation threshold: (*a*) From macroscopic cement paste strength data [8]; (*b*) nanoindentation modulus data [9]; (*c*) nanoindentation hardness data [9]. The curved thin lines in figure (*b*) are obtained using Sanahuja et al.'s elasticity model for different oblate aspect ratios (from left to right) $r^s = 1/100$; 1/10; 1/4; 1/2 (for $n^s = 1/5$).

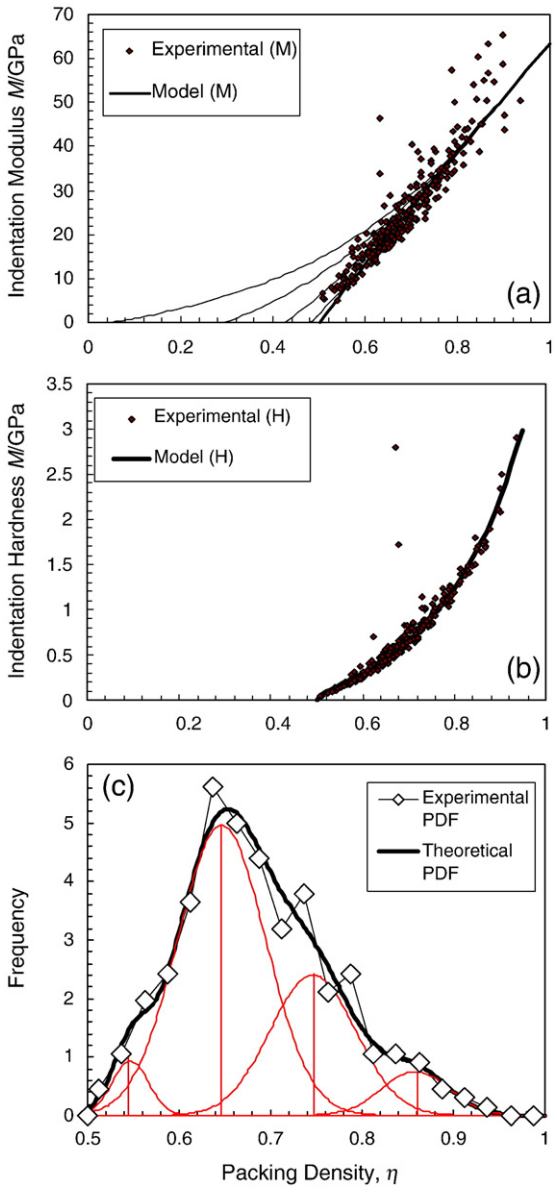

Fig. 3. Frequency vs. packing density distribution of hydration products (c), based on the scaling of (*M*,*H*) with the packing density (*a*,*b*). Results are based on 300 nanoindentation tests of hardened *w*/*c*=0.5 white cement paste [20]. The curved thin lines in figure (*a*) are obtained using Sanahuja et al.'s elasticity model for different oblate aspect ratios (from left to right) r^s=1/100; 1/10; 1/4; 1/2 (for n^s=1/5).

the particles can be fixed at around 4 nm, which are locally randomly packed in the LD structure. The particles scatter as if they are spherical and it is important to note that when the particles deviate from spherical, such as when C–S–H is decalcified, the SANS data deviates significantly from the model fit [18]. The same observation holds for the early-age behavior of C–S–H [19]; that is, while the packing density is a kinetics parameter – low density during the first 30 or so hours – high density during the diffusion controlled later on – SANS data does not support a change of shape with time.

4. C–S–H packing density distributions in hardened cement paste

A refined analysis of the packing density of the hydration products in hardened cement pastes is achieved by scaling indentation modulus and indentation hardness obtained on a large array of indentation tests by means of linear and non-linear micromechanics models. The approach developed and validated in [20] supports the assumption of a random amorphous packing of the C–S–H hydration products, by scaling indentation modulus *M* (which relates to elasticity properties, [21,22]; Fig. 3(*a*)) and indentation hardness *H* (which relates to strength properties, [23,24]; Fig. 3(*b*)) with the packing density. This type of approach provides a means of assessing the distribution and volume fractions of each packing density of hydration products in the hardened cement paste material — without a priori assumptions. A typical example is shown in Fig. 3 highlighting the existence of four possible packing densities of the same elementary particles [20]: a random-loose packed arrangement, close to the random-loose packing of uniform spheres of 0.555±0.005; the LD C–S–H arrangement with a characteristic packing of 0.65±0.05 (Mean±St. dev. of Gaussian deconvolution in Fig. 3); the HD C–S–H arrangement with a characteristic packing of 0.75±0.05, and finally an Ultra-High Density C–S–H phase whose packing density 0.86±0.04 comes remarkably close to a two-scale random spherical limit packing of η=0.64+(1−0.64)×0.64=0.87.

5. Closure: Does C–S–H particle shape matter?

This brings us back to the question: Does C–S–H particle shape matter? It is the merit of Sanahuja et al.'s inspiring contribution to demonstrate that while the particle shape affects the percolation threshold (Fig. 1), its influence on mechanical properties for highly packed systems is truly of second order as soon as the packing density is above the random-loose packing fraction of uniform spheres. Figs. 2(*b*) and 3(*a*) indeed confirm for oblates, what Sanahuja et al. note for prolates (Fig. 7 in Sanahuja et al.'s paper). This pattern seems to be a general characteristic of all types of hydrated nanocomposites, including C–S–H, hydroxyapatite (HA) in bones and compacted clay particles. In fact, as Fig. 4 shows, all those materials exhibit an almost linear scaling of their elasticity properties through a percolation threshold well approximated by η_0=0.5, despite their visual particle shape (~1/25–1/20 for clay particles [25,26]; ~1/25–1/10 for plate or needle shaped crystals of impure HA [27,28]; or the needle to fibrillar morphology of C–S–H inner and outer products visible by e.g. TEM [29]). Otherwise said, given their typical high packing density, micromechanics alone cannot resolve order in the particle shape when understanding and predicting the mechanical response of hydrated nanocomposites. Thus, it seems to us prudent to consider the influence of the particle shape as negligible in linking mechanical properties to microstructure of hydrated nanocomposites, including cement-based materials.

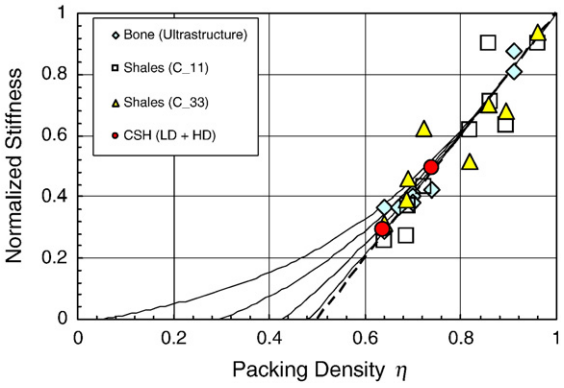

Fig. 4. Normalized stiffness vs. packing density data, determined from mineralogy data: Bone data from the compilation of experimental data by Hellmich et al. [31] (based on data from Lees et al. [33] and Lees and Rollins [32]); Shale data from compilation of data by Ortega et al. [34]. The linear scaling represents a spherical morphology (r^s=1, η_0=0.5; Poisson's ratio n^s=1/5 [9]). The curved thin lines are obtained using Sanahuja et al.'s model for different oblate aspect ratios (from left to right) r^s=1/100; 1/10; 1/4; 1/2 (for n^s=1/5).

In return, considering a spherical shape in a micromechanical morphology representation (i.e. η_0=0.5) effectively comes to admit that particle-to-particle forces are transmitted over randomly oriented particle-to-particle contact surfaces [30]. This randomness reflects the very nature of the hydration kinetics in hydrated nanocomposites: particles which precipitate randomly in an over-saturated solution, grow until their growth is affected by neighboring particles, generating contact surfaces. Since both precipitation and growth are random, that is without an orientational bias (except for the single layer adjacent to a clinker grain), the contact surfaces are randomly oriented as well. Despite their visible aspect ratio, the percolation threshold η_0=0.5 testifies to the randomness of the orientation of the contact surfaces between particles, establishing a unique nanogranular signature of hydrated nanocomposites (Fig. 4).

Acknowledgement

Special thanks to J. Alberto Ortega, Matthieu Vandamme, Benjamin Gathier and Chris Bobko at M.I.T. for comments and suggestions, and for implementing Sanhuja et al.'s model in MATLAB providing the model predictions for this Discussion.

References

[1] G.Y. Onoda, E.G. Liniger, Random loose packings of uniform spheres and the dilatancy onset, Phys. Rev. Lett. 64 (22) (1990) 2727–2730.
[2] B.J. Buchalter, R.M. Bradley, Orientational order in amorphous packings of ellipsoids, Europhys. Lett. 26 (3) (1994) 159–164.
[3] D. Coelho, J.F. Thovert, P.M. Adler, Geometrical and transport properties of random packings of spheres and aspherical particles, Phys. Rev. E 55 (2) (1997) 1959–1978.
[4] J.D. Sherwood, Packing of spheroids in three-dimensional space by random sequential addition, J. Phys., A Math. Gen. 30 (24) (December 21 1997) L839–L843.
[5] A.V. Hershey, The elasticity of an isotropic aggregate of anisotropic cubic crystals, ASME J. Appl. Mech. 21 (1954) 236–240.
[6] E. Kröner, Berechnung der elastischen Konstanten des Vielkristalls aus den Konstanten des Einkristalls, Z. Phys. 151 (1958) 504–518.
[7] A. Zaoui, Continuum micromechanics: survey, J. Eng. Mechanics-ASCE 128 (8) (2002) 808–816.
[8] G.J. Verbeck, R.H. Helmuth, Structures and physical properties of cement paste, 5th Int. Congress Cement Chmstry, Tokyo, Japan, 1969, pp. 1–44.
[9] G. Constantinides, F.-J. Ulm, The nanogranular nature of C–S–H, J. Mech. Phys. Solids 55 (1) (2007) 64–90.
[10] H.M. Jennings, Colloid model of C–S–H and implications to the problem of creep and shrinkage, Mat. Struct. 37 (265) (2004) 59–70.
[11] H.M. Jennings, J.J. Thomas, J.S. Gevrenov, G. Constantinides, F.-J. Ulm, A multi-technique investigation of the nanoporosity of cement paste, Cem. Concr. Res. 37 (3) (2007) 329–336.
[12] A.J. Allen, J.J. Thomas, H.M. Jennings, Composition and density of nanoscale calcium–silicate–hydrate in cement, Nat. Materials 6 (4) (APR 2007) 311–316.
[13] R.J.M. Pellenq, H. Van Damme, Why does concrete set?: the nature of cohesion forces in hardened cement-based materials, MRS Bull. 29 (5) (2004) 319–323.
[14] H.M. Jaeger, S.R. Nagel, Physics of granular state, Science 255 (5051) (1992) 1523–1531.
[15] A. Donev, I. Cisse, D. Sachs, E.A. Variano, F.H. Stillinger, R. Connely, S. Torquato, P.M. Chaikin, Improving the density of jammed disordered packings using ellipsoids, Science 303 (2004) 990–993.
[16] N.J.A. Sloane, Kepler's conjecture confirmed, Nature 395 (1998) 435–436.
[17] A.J. Allen, Time-resolved phenomena in cements, clays and porous rocks, J. Appl. Crystallogr. 24 (1991) 624–634.
[18] J.J. Thomas, J.J. Chen, A.J. Allen, H.M. Jennings, Effects of decalcification on the microstructure and surface area of cement and tricalcium silicate pastes, Cem. Concr. Res. 34 (2004) 2297–2307.
[19] A.J. Allen, R.C. Oberthur, D. Pearson, P. Schofield, C.R. Wilding, Development of the fine porosity and gel structure of hydrating cement systems, Philos. Mag. B 56 (3) (1987) 263–268.
[20] F.-J. Ulm, M. Vandamme, C. Bobko, J.A. Ortega, K. Tai, C. Ortiz, Statistical indentation techniques for hydrated nanocomposites: concrete, bone, and shale, J. Am. Ceram. Soc 90 (9) (2007) 2677–2692.
[21] L.A. Galin, Contact Problems in Theory of Elasticity. Translated by H. Moss. Edited by I.N. Sneddon, North Carolina State College (1961).
[22] I.N. Sneddon, The relation between load and penetration in the axi-symmetric Boussinesq problem for a punch of arbitrary profile, Int. J. Eng. Sci. 3 (1965) 47–57.
[23] F.P. Ganneau, G. Constantinides, F.-J. Ulm, Dual-indentation technique for the assessment of strength properties of cohesive–frictional materials, Int. J. Solids Struct. 43 (6) (2006) 1727–1745.
[24] S. Cariou, F.-J. Ulm, L. Dormieux, Hardness-packing density scaling relations for cohesive–frictional porous materials, J. Mech. Phys. Solids 56 (2008) 924–952.
[25] B. Hornby, L. Schwartz, J. Hudson, Anisotropic effective medium modeling of the elastic properties of shales, Geophysics 59 (10) (1994) 1570–1583.
[26] F.-J. Ulm, Y. Abousleiman, The nanogranular nature of shale, Acta Geotech. 1 (2) (2006) 77–88.
[27] S. Weiner, H.D. Wagner, The material bone: structure – mechanical function relations, Ann. Rev. Mater. Sci. 28 (1998) 271–298.
[28] C. Hellmich, F.-J. Ulm, Are mineralized tissues open crystal foams reinforced by crosslinked collagen? Some energy arguments, Journal Biomech. 35 (9) (2002) 1199–1212.
[29] I.G. Richardson, Tobermorite/jennite- and tobermorite/calcium hydroxide-based models for the structure of C–S–H: applicability to hardened pastes of tricalcium silicate, β-dicalcium silicate, Portland cement, and blends of Portland cement with blast-furnace slag, metakaolin, or silica fume, Cem. Concr. Res. 34 (2004) 1733–1777.
[30] C. Bobko, F.-J. Ulm, The nanomechanical morphology of shale, Mech. Mater. 40 (2008) 318–337.
[31] C. Hellmich, J.F. Barthelemy, L. Dormieux, Mineral-collagen interactions in elasticity of bone ultrastructure — a continuum micromechanics approach, Eur. J. Mech. A-Solids 23 (5) (2004) 783–810.
[32] S. Lees, F.R. Rollins, Anisotropy in hard dental tissues, J. Biomech. 5 (1972) 557–566.
[33] S. Lees, D. Hanson, E.A. Page, Some acoustical properties of the otic bones of a fin whale, J. Acoust. Soc. Am. 99 (4) (1995) 2421–2427.
[34] J.A. Ortega, F.-J. Ulm, Y. Abousleiman, The effect of the nanogranular nature of shale on their poroelastic properties, Acta Geotech. 2 (3) (2007) 155–182.